Sustainable Energy & Fuels

ROYAL SOCIETY OF CHEMISTRY

PAPER

View Article Online
View Journal | View Issue

Cite this: *Sustainable Energy Fuels*, 2020, **4**, 3764

Big problem, little answer: overcoming bed agglomeration and reactor slagging during the gasification of barley straw under continuous operation†

Hassan A. Alabdrabalameer,[a] Martin J. Taylor, *[ab] Juho Kauppinen,[c] Teemu Soini,[cd] Toni Pikkarainen[c] and Vasiliki Skoulou *[ab]

Received 30th January 2020
Accepted 25th May 2020

DOI: 10.1039/d0se00155d

rsc.li/sustainable-energy

Defluidisation as a result of reactor bed agglomeration is a global challenge associated with the gasification of lignocellulosic biomass waste, specifically its high inorganic content. The use of conventional water leaching has been scrutinised for the removal of inorganic constituents from barley straw, a highly abundant waste feedstock with a high ash content. The resulting pre-treated material was subsequently gasified at 750 °C and 850 °C under continuous flow, where it was found that bed agglomeration as a result of the ash melting induced mechanism can be eliminated, as visualised by SEM and EDX studies. Here, the presence of eutectic mixtures result in the fusing of a SiO_2 rich bed material that causes a sudden pressure drop in the reactor, resulting in a forced shutdown. Leached barley straw was found to effectively solve this issue and sustained gasification for a long period of time, as well as limiting inorganic based decoration on the surface of bed material grains after reaction. Additionally, leaching was found to enhance the production of low carbon fuel gases where an improved product yield of 31.9 vol% and 37.3 vol% for CO and CH_4 was observed at 850 °C, as compared to untreated equivalent.

Introduction

In the race to reverse global warming damage and eliminate the use of fossil based fuels, lignocellulosic biomass derived wastes are an attractive, alternative approach to produce low carbon energy *via* thermochemical processes such as pyrolysis and gasification.[1,2] Specifically, the use of 'fast growing' lignocellulosic waste such as straws, while not competing with food and fuel markets, are the true sustainable answer to the global energy crisis. This is important especially as when waste-to-energy production technologies are coupled with Carbon Capture and Storage (CCS) or Utilisation (CCSU) technologies, leading to net CO_2 emissions being negated.[3,4] Repurposing such wastes as alternative and 'green' solid fuels are further beneficial to the environment by releasing far lower emissions (CO_2, NO_x, SO_x and heavy metals) and various other pollutants when compared to traditional fossil based fuels such as coal.[1,3,5–7] Currently, woody biomass is the dominant variant used for generating energy *via* combustion, as a result the demand and the cost has increased over recent years.[7] Due to the heightened demand of this type of solid biofuel in global markets, there has been a drive to exploit other potential lignocellulosic biomass feedstocks to offset the strain on acquiring a singular waste stream, one alternative are herbaceous wastes such as straws.[1,7] Comparing both types of lignocellulosic waste, straws have a much lower bulk density, higher mineral or ash content and a fibrous structure, often possessing a higher lignin content.[7,8] However, this form of lignocellulosic waste is considered problematic due to its inherently high alkali and alkaline earth metal (*e.g.* Na, K, Ca and Mg) content.[2,4,8–10] The inorganic content in the non-woody biomass is higher than woody equivalents by 5–20 times which leads to various operational downstream issues such as, bed agglomeration, reactor corrosion/slagging and de-fluidization during thermochemical reactions for syngas and bio-oil production.[4,7,11]

Generally, the most common form of reactor technology used in thermochemical downstream processing of coal and lignocellulosic waste is the fluidized bed system. This is where a usually inert bed material composed of various oxides is used to increase the solids mixing rates and heat transfer to the feedstock.[10,12–16] The transition between adapting fluidised beds previously used for coal to biomass waste for power generation is minimal due to the fuel flexibility and high combustion

[a]*B*[3] *Challenge Group, Department of Chemical Engineering, University of Hull, Cottingham Road, Hull, HU6 7RX, UK. E-mail: V.Skoulou@hull.ac.uk*

[b]*Energy and Environment Institute, University of Hull, Cottingham Road, Hull, HU6 7RX, UK. E-mail: Martin.Taylor@hull.ac.uk*

[c]*VTT Technical Research Centre of Finland Ltd, Renewable Energy Processes, Espoo, Finland*

[d]*Reteres Oy, Kytömaantie 32, 41390 Äijälä, Finland*

† Electronic supplementary information (ESI) available. See DOI: 10.1039/d0se00155d

efficiency.[10,13,17–19] Fluidized bed reactors provide lower emissions, low temperature operation, better heat transfer, solid/gas mixing and as a result a large surface area for an upward flowing gas stream.[10,13,15,18,20]

Not without issues, the fluidised bed reactor, especially beds made from silica sand, can suffer from 'bed agglomeration'. This phenomenon has been reported over the last 30 years for generating energy from lignite.[15,17,19–21] Bed agglomeration occurs when ash components from the biomass feedstock interacts with the bed material, due to lower melting temperature of ash compounds opposed to oxides, layers and agglomerates form restricting gas flow and subsequently reactor bed destabilisation and collapsing as a result of defluidisation.[14,15,22–24] Alkali metals in the biomass waste form eutectic mixtures in the liquid phase that deposit on the surface of the bed material grains and form a physical linkage between the bed particles which leads to bed agglomeration *via* alkali silicate (molten) bridges, fusing the bed material particles together.[13,15–17,23] As a prelude to de-fluidisation there is a decrease in the heat transfer and the bed hydrodynamics which influence the temperature distribution throughout the reactor.[13,18,25] As a cascade process, a steady or sharp decrease in the reactor pressure can be detected due to an unstable bed temperature.[10,13,26] This process leads ultimately to a full reactor shut down where the bed material must be replaced and the reactor cleaned of slag deposits. The costs associated with production stoppages and the reactor's cooling decrease the efficiency of the generation energy from various low quality types of lignocellulosic biomass waste. As a result of the stop–start behaviour and corrosive nature of some of the inorganic deposits, the lifespan of the equipment and reactor on a whole are radically decreased.[10,17,27]

The occurrence of bed agglomeration is highly dependent on the inorganic composition of the biomass feedstock, specifically alkali metals, in conjunction with the reactor operating temperature and reaction atmosphere.[13,17,21,22,28,29] The most problematic elements that participate in bed agglomeration are K, S, Cl and P, this is because they can form low melting point compounds with the bed material.[27,30–35] From the list of elements mentioned, the most troublesome is K, this is due to its reactivity and ability to form low temperature eutectic mixtures with Si, a common/cheap major component in bed materials which have much lower melting point than SiO_2 (1710 °C). The combination of these two elements in various stoichiometries can produce a material which has a melting point as low as 764 °C.[14,22,27,30,35–37] The presence of Cl enhances the mobility of K by forming KCl slag deposits on cold spots on the reactor walls.[14,20,27,29,38] Straws generally possess a high Na and K content which will be more likely to form bed agglomerates. However, solid fuels with a high concentration of Ca will decrease this tendency with Si.[20,21,25,27,32] For formed alkali silicate mixtures, residual S can facilitate a further decrease in melting temperature to around 700 °C. This means that such bed agglomeration is possible for combustion, low temperature gasification and pyrolysis conditions.[11,15,25,38] The stoichiometry of eutectic mixtures can be varied by the inherent Si content in the waste feedstock. Specifically with K, variations in the composition will generate molecular structures such as $K_2O{\cdot}SiO_2$, $K_2O{\cdot}2SiO_2$, $K_2O{\cdot}3SiO_2$ and $K_2O{\cdot}4SiO_2$ which have congruent melting points of 976 °C, 1015 °C, 740 °C and 764 °C, respectively.[6,10,11,20,25,38] This infers that a high Si content specifically in a 3 : 1 or 4 : 1 molar ratio should be avoided, to limit eutectic melting. However, the addition of Ca in SiO_2, forming Ca_2SiO_4 (calcium silicate) has a higher melting point of 2130 °C in comparison to K_2SiO_3 which has been found to undergo eutectic melting at 780 °C.[15,25,38,39]

Previously, the literature characterization of reactively formed agglomerates have been found to be formed in a layered morphology, where agglomerates containing higher K concentrations have a larger array of layers.[21,25,34,36,40] These agglomerations are formed in a heterogeneous fashion due to the presence of hot spots inside the fluidised bed reactor that may reach in excess of 1000 °C.[25] Prior to interacting with the bed material, the Si and K in the lignocellulosic biomass waste can create a transient eutectic entity during the thermochemical reaction before going on to interact with the bed material, this is called melting induced agglomeration. The mechanism of this process begins by forming a molten char (carbon from the feedstock) that collides with bed particles and fuses them together. After decomposing the char, the Si rich bed material particles will remain linked together *via* the inorganic 'glue'.[21,22,24,27,36,40] The coating mechanism depends on the bed material composition, the melting induced mechanism depends solely on the fuel ash composition.[17,24,27,36,40] Decreasing the tendency of the bed agglomeration can be achieved by utilising various other bed materials that will reduce the reactivity of alkali components in the feedstock's ash, alternatively co-firing/blending different feedstocks or reduce/remove problematic elements *via* a pre-treatment protocol.[23,25,41]

One of the most common and cheap bed materials is SiO_2 (silica sand). However, due to the reasons mentioned previously, using a silica bed in biomass gasifiers increases the tendency of bed agglomeration. Adding elements to the bed material such as Mg, Al, and Ca have been found to reduce the formation of Si based eutectic linkages with K.[14,15,31,38,41,42] Other common bed materials used previously for fluidized bed reactors are alumina, olivine, magnesite, feldspar, dolomite and limestone.[15,31] However, each of these materials contribute a higher operating cost to the process as compared with SiO_2 sand alone.[15,31,38,42] A low cost and efficient method of removing problematic inorganic components from the feedstock is *via* leaching or otherwise known, water washing.[3,17,43,44] Typically, leaching is carried out in demineralised water, due to the solubility of K in this medium the rate of extraction is the highest than for any other element. Other elements with a high affinity for removal *via* leaching are Na and Ca whereas P, Mg, Fe and S are much slower due to possessing far higher solubility values.[3,7,42,43]

In this work, we will be investigating the effect of leaching on the removal of ash constituents from barley straw, a feedstock naturally rich in ash. Subsequently, this feedstock will be tested in a continuously fed fluidised bed reactor under gasification conditions, both in a raw and leached form. Here, the melting induced mechanism will be probed to ascertain whether bed

agglomeration occurs and if so, to what extent do inorganic deposits decorate the surface of the bed material under varying operational temperatures. Finally, the leaching process's effect on the reaction selectivity in the production of low carbon gaseous fuels will be examined.

Materials and methods

Preparation and characterisation of barley straw

For this work, due to its abundancy in the United Kingdom, barley straw has been used as the fuel source for gasification. This fuel is a suitable candidate to generate defluidisation problems due its naturally high concentrations of inorganic elements, Table 1. Initially, the barley straw was milled using a Retsch GM200 Grindomix Knife Mill followed by sieving fractions of the desired particle size (1–2 mm) using a Retsch AS200 Vibratory Sieve Shaker. Leaching was carried out using deionised water for 24 h (700 rpm) at a ratio of 15g L^{-1} using a Heidolph Hei-Tec hotplate at 25 °C, the temperature was monitored by a Pt1000 stainless steel thermocouple placed in the leachate. The materials were filtered and dried under *vacuo* before drying in a Fisherbrand gravity convection oven for 24 h at 105 °C.

The ultimate, proximate and elemental analysis of the raw and leached barley straw can be seen in Table 1. The ultimate analysis of both raw and leached barley straw was carried out according to SFS-EN ISO 16948, 16993 and 16994 standards.

Table 1 Characterization of the untreated and leached barley straw

	Untreated barley straw	Leached barley straw
Ultimate analysis (wt% dry basis)		
Carbon	42.2	44.3
Oxygen[a]	51.1	49.3
Hydrogen	5.8	5.9
Nitrogen	0.8	0.5
Sulphur	0.1	N/D[b]
Proximate analysis (wt% dry basis)		
Moisture	7.4	3.5
Volatiles	79.5	85.7
Fixed carbon	9.8	10.2
Ash	3.3	0.6
Elemental analysis (ppm)		
Cl	970	80
K	12 500	1600
Na	170	28
P	200	55
Ca	2600	1300
Al	21	12
Mn	12	5.8
Cu	1.4	0.74
S	810	230
Mg	370	140
Si	890	860

[a] Calculated by the difference. [b] N/D – not detected.

The proximate analysis took place under N_2 flow in a thermogravimetric analyser according to SFS-EN ISO 18134-2, 18123 and SFS-EN ISO 18122 standards. Ash composition was measured using an ICP-OES (SFS-EN ISO 11885) method, except Cu which was measured using ICP-MS (SFS-EN ISO 17294-2). Residual Cl concentration was determined by an Ion Chromatograph (SFS-EN ISO 10304-1). Table 1 shows that there has been a substantial change to the inorganic composition of the barley straw where 76.8% has been removed; this is very close to the value calculated by the proximate analysis of 81.8 wt%.

Characterisation of reactor bed material

For this work the bed material considered is silica sand, this was due to the tendency of undergoing bed agglomeration and applicability to current practices. By utilising a particle size of 250–500 μm, there is a range of smaller and larger grains which have the potential of agglomerating *via* low melting point eutectic mixtures. The bed material was characterised before and after the thermochemical reactions at varying temperatures (750 °C, 850 °C and 920 °C). Scanning Electron Microscopy (SEM) images were acquired *via* a Zeiss EVO 60 instrument and Oxford Instruments Inca System 350 under the pressure of 10^{-2} Pa and an electron acceleration voltage of 20 kV. Prior to imaging, the bed materials were sieved to only consider particles that had a diameter larger than the unused bed material, powders were adhered to a coated conductive carbon tape and attached to the specimen holder, where a 10 nm thick coating of graphite was added to the surface. The composition of the bed material as determined *via* Energy Dispersive X-ray Spectroscopy (EDX) found the silica sand to contain Si (57.1 wt%), Al (22.1 wt%), Na (18.9 wt%), K (0.8 wt%), Ca (0.8 wt%) and Fe (0.3 wt%). Powder X-ray Diffraction was carried out using a Philips X'Pert MPD diffractometer. An unused bed material diffractogram is shown in Fig. S1† showing a well resolved pattern where reference markers to SiO_2 and aluminium silicates are shown.

Although seen as a relatively fast process, leaching was carried out over a sustained period to maximise the removal of all elements. It has been found in the literature that elements such as Si, Al and Ti have a low water solubility and require high temperatures or the use of acid for effective removal.[43,45] On the other hand elements such as K, Na, S and Cl are soluble in water and are rapidly removed.[43,45,46] Of the extracted elements there has been a 91.8% reduction in Cl, 87.2% reduction in K, 83.5% reduction in Na and 71.6% reduction in S. However, there has only been a reduction of 3.4% for Si, the extraction of this element is known to be temperature dependant. It was found that leaching at 90 °C was more effective than leaching under mild conditions (as conducted in this work), increasing the efficiency of removal up to 65%.[46] The removal of K to such a degree has radically altered the Si : K molar ratio from 0.1 to 0.75, a higher value means a substantial decrease in the potential of generating a eutectic mixture derived from Si–K. All of the other elements monitored were decreased by at least 40%. Additionally, by drying the feedstock post leaching, the recorded moisture content was decreased by 52.7%.

Thermochemical transformation

Fig. 1 shows a schematic of the bench-scale Bubbling Fluidised Bed (BFB) reactor system used routinely for combustion experimentation. However, for this work it was customised to operate under gasification conditions (hypo-stoichiometric oxygen preventing complete combustion) this type of reactor has been effectively used for agro-waste gasification in the past.[47] The thermochemical conversion of barley straw was carried out in the BFB reactor with a 0.9 m high riser and a diameter of 0.037 m, reactor operational conditions are reported in Table S1†. The BFB system was installed with an electrical temperature stabilisation unit and the gas feeds were regulated *via* a Environics Series 4000 Multi-Component Gas Mixing System to mix and optimise the stream composition and flow rate of O_2 and N_2, feeding from the bottom of the reactor at a flow rate of 6 L min^{-1}. This corresponds to a gasification medium superficial velocity ranging between 0.36 and 0.42 m s^{-1}. For gasification, the temperature was controlled with fine precision between 750 °C to 920 °C, monitored by six thermocouples 30 mm, 100 mm, 300 mm, 450 mm, 600 mm and 669 mm above the grid level. The first two measurement points are in bed area and the four upper are in the freeboard area. The thermal output of the furnace was linked with a PID system that monitors and regulate temperature while observing pressure increases/decreases in the BFB reactor, just below the grid, leading to blockages or defluidization because of bed agglomeration. Fuel gases and other emissions produced from the reaction in the form of a producer gas was analysed *via* an on-stream FTIR gas analyser system. The product gases monitored were H_2O, CO, CO_2, CH_4, SO_2, NO, C_2H_6, C_2H_2 and C_2H_4 as well as other trace residuals. As gasification was the thermochemical downstream process used, the oxygen content in the stream was 1 vol%. The produced emissions and particulates were released from the top of the BFB reactor *via* the particulate trapping cyclone system after a temperature adjustment to 180 °C (as shown in Fig. 1), this was subsequently fed into the FTIR system for analysis. To remove tar from the producer gas it was flowed through a series of traps containing a water/propan-2-ol mixture submerged in ice.

Defluidisation and bed agglomeration tests

To assess the effect of water leaching on bed defluidisation during the gasification of barley straw, the reactor utilised a continuous feeding system. This is where untreated and pre-treated straw was hopper fed *via* a screw feeder at a rate of 15–100 rounds per minute (rpm). The screw feeder speed was increased by 10 rpm variably over time to sustain a constant flow. During the initial reactor pre-heating process, 26 g of silica bed material was added. Once at the desired temperature set point, the straw feeding began, increasing in feed rate as the reaction progressed. Using this approach, both de-fluidisation

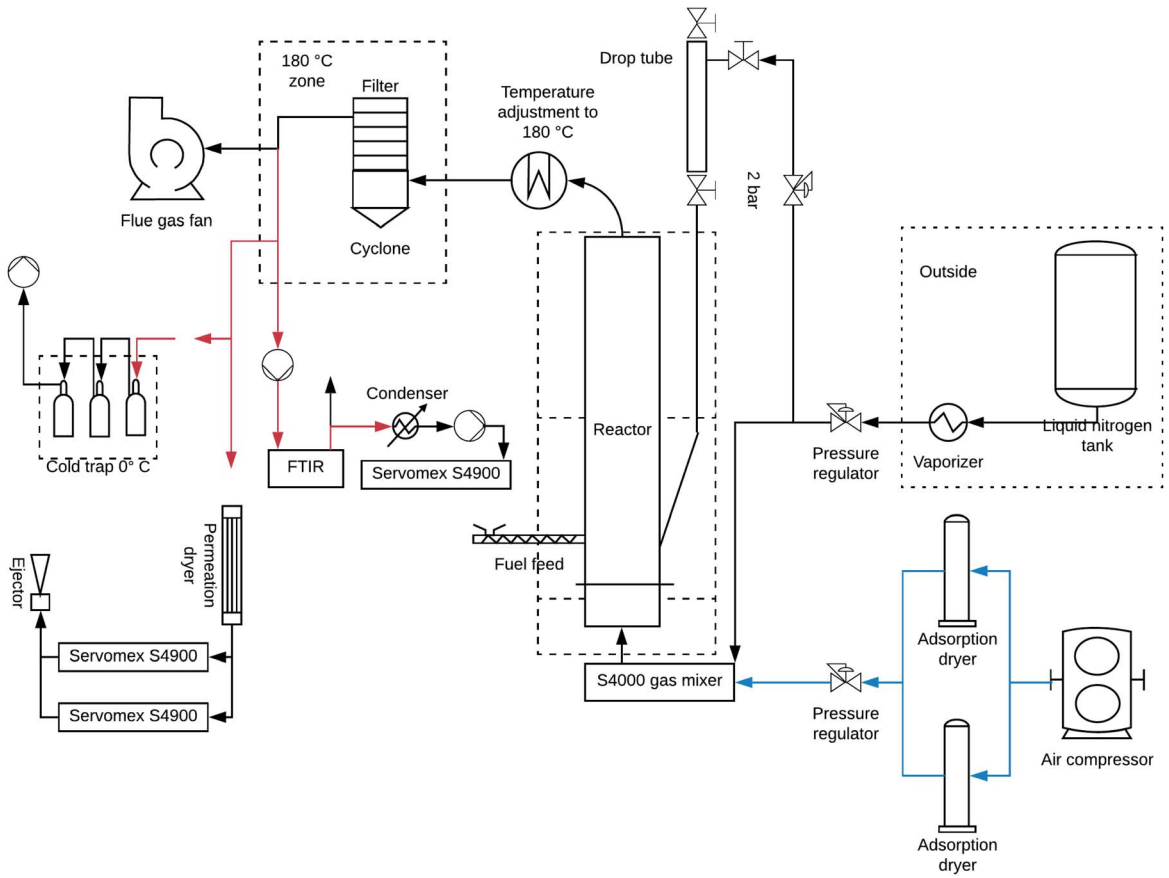

Fig. 1 Schematic representation of the biomass waste, bench scale Bubbling Fluidized Bed (BFB) reactor system.

and bed agglomeration tests were carried out for untreated and pre-treated materials. This is where 2.4–23.3 g of straw was added depending on whether a pressure drop in the bed was detected. If a sharp pressure drop was detected or a fluctuation in temperature as a result of de-fluidisation, the reactor was shut down. For this process, the output followed is the time taken until experimental breakdown or rate of bed agglomeration. This was measured from the time the feedstock feed began to the time the reactor was shut down. The producer gas monitored during the time the reactor was active was collected to understand the behaviour, thermal efficiency, reactivity and emissions of both untreated and leached barley straw. After the reactor was cooled, the bed material was recovered and sieved gently for further characterisation. Instead of using the vibratory shaker (used for fractioning barley straw), the sieves were gently moved side to side by hand as to not physically disrupt the agglomerated bed material.

The bed agglomeration tests were carried out across five different scenarios, where the gasification temperature and waste pre-treatment were varied, this data is summarised in Table 2. In Table 2, not only were temperature and pre-treatment considered but also the maximum input speed and subsequent agglomeration time (time until a sudden pressure drop was recorded). It is clear that the untreated barley straw suffered from de-fluidisation overtime where gasification at 750 °C and 850 °C had very similar times of agglomerate formation (32 and 41 min, respectively). For the highest temperature, 920 °C, this was vastly faster at 19 min. Due to operational difficulties in feeding untreated barley straw into the fluidized bed reactor, there was substantially less material added over the experiment *via* a slower feed rate than its leached counterpart. The leached barley straw was not only added seamlessly, but also flowed smoothly into the screw feeder and could be fed at a much higher feed rate, where 45 rpm was the nominal rate of feeding. As a result, ~20 g of pre-treated barley straw was added over 1 h. This feedstock presented a sustained pressure (Fig. 2) for both temperatures. The mass input for temperatures 750 °C and 850 °C were 2.3× and 4.4× greater for the leached materials than for raw barley straw. In fact, this addition could have been far higher as the reactor had reached a constant stable pressure during feeding, ending only due to exhausting the hopper.

Fig. 2 depicts the effect of temperature on the rate of bed agglomeration. This is where the gasification reactor sustains a steady pressure until a sudden drop is observed after the period described in Table 2. Unlike reactions at 750 °C and 850 °C there was no indication of bed agglomeration at 920 °C until an immediate drop, this means that the formation of eutectic mixtures and the fusing of the bed material occurs at a much faster rate than for the lower temperature reactions. For the lowest operational temperature (750 °C) this was recognisable by a steady drop in pressure over 6 min before an immediate drop at 43 min (highlighted by a black dashed line).

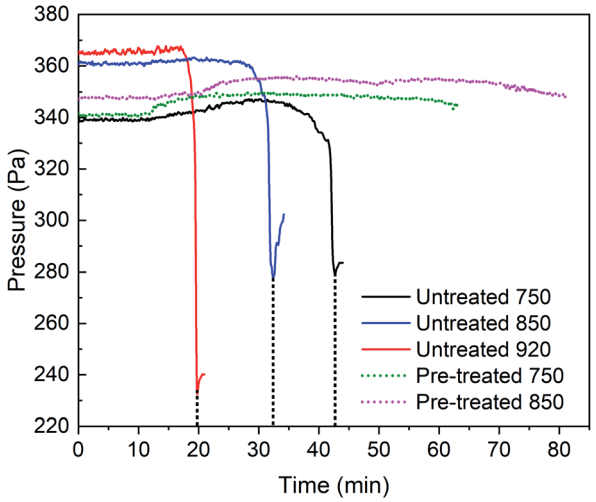

Fig. 2 The effect of gasification temperature on bed agglomeration for untreated and pre-treated barley straw (black dashes highlight the point of agglomeration).

Fig. 2 also shows the pressure profile for pre-treated barley straw where there was a sustained reaction for over 1 h, for both thermochemical reactions at 750 °C and 850 °C. The leaching process has had a clear impact on the bed stability due to the removal of K, Cl, Na, Ca and S. This improvement means that leached barley straw can be a sustainable solid fuel for gasification in the future.

To understand the extent of bed agglomeration and the effect of inorganic deposits on the bed material after gasification, SEM and EDX studies were carried out. This involves scrutiny of the surface of the bed material grains and boundaries with adjoining grains. Fig. 3 shows a low magnification view of fresh bed material, this also has a higher magnification inset image of a single grain clearly demonstrating that there are both no surface residues and no fusing between the grains overall.

Table 2 Effect of leaching barley straw waste on the rate of bed agglomeration at varied gasification temperatures

Samples	Feedstock	Temperature (°C)	Feeding rate (rpm)	Agglomeration time (min)	Mass input (g)
1	Untreated barley straw	750	15–60	43	9.4
2	Leached barley straw	750	15–100	N/D[a]	21.3
3	Untreated barley straw	850	15–45	32	5.3
4	Leached barley straw	850	15–45	N/D[a]	23.3
5	Untreated barley straw	920	15–45	19	2.4

[a] N/D – no detected bed agglomeration, experimental data recording ends due to exhausting the fuel hopper.

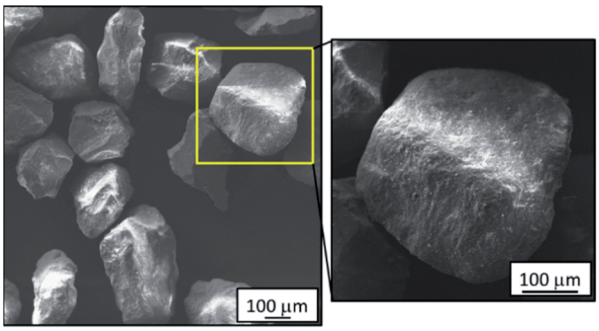

Fig. 3 The surface morphology and separation between fresh silica rich bed particles.

Fig. 4A–D show the effect of ash constituents from the raw barley straw on the bed material at 750 °C (Fig. 4A), 850 °C (Fig. 4B) and 920 °C (Fig. 4C and D). For the lowest temperature, Fig. 4A shows that on the lowest magnification image there is clear fusing between the bed material grains, this is highlighted by yellow circles at the grain boundaries. Upon magnification there is also evidence of reaction based surface decoration, by using EDX on residues it was found that the K and S in the raw feedstock has formed K_2SO_4 slag deposits (green squares) during gasification. A full EDX map of this deposit is shown in Fig. S2.† However, in other regions it was clear that there were areas of bulk surface modification from the decomposition of the barley straw. Such a region is highlighted by a blue square where an EDX spectrum was acquired, presented in the adjacent bar chart. This shows the variation of inorganic build up (K, Ca, Mg, S, P, Mn and Cr) that is not present on the fresh SiO_2 bed material (Fig. 3). There is also isolated pockets of Na and Ca based crystals (red square). Increasing the temperature to 850 °C (Fig. 4B) there is a clear difference in the surface structure of the bed material after gasification. The three images represent a stepwise increase in magnification of the parent image. Here, there is a dramatic increase in surface decoration of the bed material and agglomeration between bed grains, one

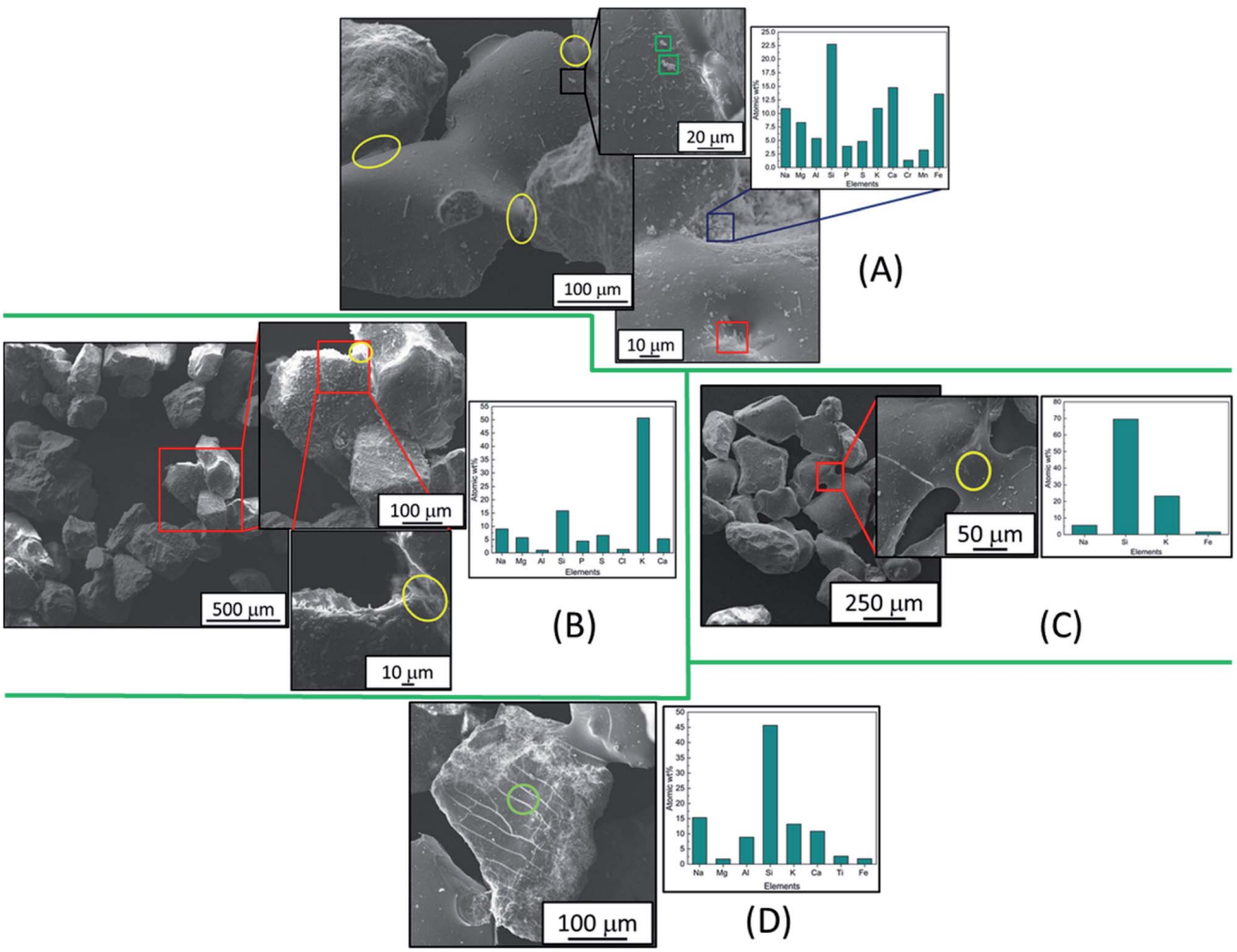

Fig. 4 HRSEM images of bed materials after the gasification of untreated barley straw where, (A) is after 750 °C, agglomeration between particles is indicated by yellow circles, green squares represent K_2SO_4 deposits, red square shows Na rich crystal deposits and the blue square indicates the point at which the EDX scan was recorded. (B) is after 850 °C, red squares show the areas of magnification and the yellow circles show the point of EDX. (C) is after 920 °C, the red square shows the resulting eutectic mixture forming a bridge between two grains, the yellow circle is the area of EDX. (D) is a different region from 920 °C where surface coating induced melting is shown with subsequent EDX data.

such join was scanned by EDX (yellow circles) which show a wide variation in elements observed including a high concentration of K and the presence of Cl. The Si : K value (Si atomic wt%/K atomic wt%) for this spot was very low, as the Si : K molar ratio decreases (more K content), the tendency of the bed agglomeration increases. Additionally, fouling and reactor corrosion will increase; surface decoration of the bed material in this image shows a large concentration of surface structures, which contain a high atomic wt% of various elements including Cl and S. This means that compounds such as KCl and K_2SO_4 were formed. Fig. 4C shows an increase in bed particles fusing together at 920 °C. Such an issue verifies why there was a sudden pressure drop in the BFB gasification reactor shown in Fig. 2. Specifically, a bridge between two particles has been imaged (red square) where a eutectic mixture with a high Si : K ratio (EDX accompanying data showing a 3 : 1 molar ratio) has been instrumental in this linkage generating a $K_2O{\cdot}3SiO_2$ mixture. Finally, Fig. 4D shows a different region from the 920 °C sample which shows a difference in the grain surface decoration. Here, the barley straw has left a large coating of inorganic material on the surface of the bed material including a detectable amount of Ti as well as high concentrations of K, Ca and Na. The large Si signal is in part due to the bare bed material.

The SEM images shown for the post reaction bed material with untreated barley straw (Fig. 4) are contrary to those shown in Fig. 5A and B for leached equivalents. Fig. 5A is the bed material from the pre-treated barley straw reaction at 750 °C. In comparison with Fig. 4A where there was grain fusing, this is not apparent for the leached material. There is also no clear surface ash deposits visible across the sample, this suggests that water washing has removed the majority of problematic ash constituents (Table 1). The EDX data shown in the graph beside Fig. 5A shows that the particle grains appear similar to unused bed material. This is echoed in Fig. 5B where there is both no surface decoration or bed material linkages, unlike the obvious agglomeration in Fig. 4B. Once again the EDX scan showed that the grains were nearly the same as unused bed material, albeit with a slightly higher Ca content. However, if this is the case would result in the formation of a calcium silicate material which has a higher melting point than Si : K mixtures. Additionally, the Si content is higher than the unused bed material; this is attributed to Si deposits from the leached barley straw (not removed using mild leaching conditions).[44]

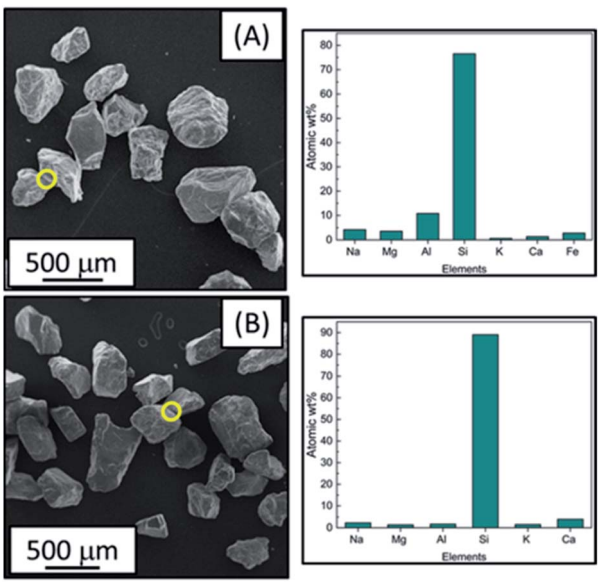

Fig. 5 The effect of gasification temperature on bed agglomeration for leached barley straw where, (A) is after 750 °C, the accompanying EDX area is marked by a yellow circle. (B) is after 850 °C, the EDX spot is indicated by a yellow circle.

Reactivity of leached barley straw under continuous flow

The effect of pre-treating barley straw on the effect of bed agglomeration during gasification has been discussed. However, the reason for investigating this is for the future development and optimization of fluidised bed energy production technologies for sustainable, highly abundant waste feedstocks such as straws. The use of straws for thermochemical processes are thwart with issues such as fouling/slagging in the reactor, feeding blockages, disruption of heat flow and defluidisation due to its low density and its ability to stick to the pipes and reactor walls. However, by water leaching, feeding and sticking issues were overcome, leading to an effective solid alternative fuel.

This work has shown that leaching barley straw is also beneficial for the production of heat producing low carbon fuels at 750 °C and 850 °C such as; CO, CH_4, C_2H_4 (ethylene) and C_2H_2 (acetylene). Fig. 6 shows the effect of leaching on the product mix and output concentration as a function of gasification temperature.

Fig. 6 clearly shows that leaching barley straw is beneficial for the production of combustible gas such as CO, CH_4, C_2H_2 and C_2H_4 at both operational temperatures. Gasification at 850 °C was found to be the optimum temperature for the production of carbon monoxide (CO) and methane (CH_4).

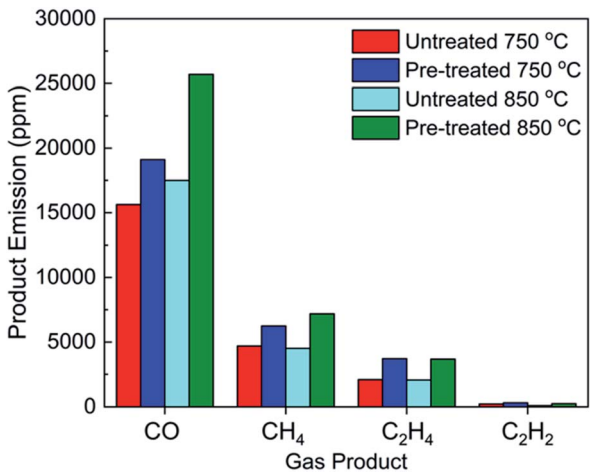

Fig. 6 Variation in the product mix and concentration in the steam depending on temperature and feedstock pre-treatment.

However, by using the lower temperature of 750 °C with the same feedstock, the product mix contains as expected more ethylene and acetylene, as under this temperature range the gasification reactions are inhibited in favour of pyrolysis. The effect of leaching the feedstock led to an increase in CO production by 18.2% and 31.9% for 750 °C and 850 °C, respectively as compared with gasification reactions at the same temperatures using raw barley straw. Leaching straw had a profound benefit for the production of CH_4 across both temperatures. There was a 24.8% and 37.3% increase compared with the raw feedstock at 750 °C and 850 °C, respectively. The largest increase was for the production of acetylene at 850 °C where an increase of 62.6% was monitored after leaching. The various increases in fuel gas production is attributed to the disruption of intermolecular interactions within the crystalline cellulose of the feedstock. This would mean that the feedstock is more susceptible to thermochemical decomposition, as less energy would be required to initiate a reaction as the crystallinity index of the cellulose has been lowered.[44,48] Additionally, a decrease in inorganic content could be attributed to a beneficial increase in low carbon fuel production by increasing the heating value of the biomass waste.[49] Ultimately, the removal of ash constituents has led to a sustainable process where subject to sufficient solid fuel, the gasification of pre-treated barley straw is a long term option for the production of low carbon gaseous fuels, where bed agglomeration and straw feeding problems have been eliminated.

Conclusions

Fluidised bed reactor bed agglomeration has been scrutinised for the gasification of a highly abundant lignocellulosic biomass waste material rich in ash, barley straw. The bed agglomeration phenomena is a global challenge that prevents the continuous operation for waste to energy systems and utilization of low carbon solid fuels. This leads ultimately to high cost solutions, casting a shadow on the use of waste gasification as a green and environmentally friendly answer to the energy crisis. This work has found that a traditional pre-treatment technique (leaching) used for coal, can be adapted and proven beneficial for lignocellulosic wastes that are rich in ash. This pre-treatment decreased the ash composition by ~80% after 24 h. This was found to eliminate the formation of eutectic mixtures between Si and K when operating at 750–850 °C under a dilute O_2 atmosphere, where mixtures with a high Si : K molar ratio will form low melting point linkages in the form of $K_2O{\cdot}3SiO_2$ or $K_2O{\cdot}4SiO_2$ between 740–764 °C. Such mixtures form bridges between silica bed particles and prevent produced gas from travelling through the reactor bed, leading to a pressure drop and subsequent destabilisation/reactor shutdown, a high cost problem for the bioenergy industry. It is shown that the melting induced mechanism forms varying levels of bed particle surface decoration. The surface deposits are also those known to be similar to those found in reactor slag deposits. Characterising such coatings found isolated K_2SO_4, as well as larger inorganic deposits containing K, Ca, Ti, Cl, S, Cr and Mn. Additionally, the effect of leaching was found to enhance the production of fuel-based gases during gasification, where there was a 31.9% and 37.3% increase in the production of CO and CH_4 when operating at 850 °C under continuous flow. Concluding that not only is bed agglomeration eliminated but also the feeding challenge was overcome, thus the production of low carbon fuels from lignocellulosic waste is dramatically improved.

Conflicts of interest

There are no conflicts to declare.

Acknowledgements

HAA and VS would like to thank the BRISK2 Project (Horizon 2020 research and innovation programme, grant: 731101), VS and MJT would like to thank EPSRC for funding part of this project (EPSRC New Investigator Grant) former First Grant, (EP/P034667/1) as well as partial funding through the THYME project (UKRI, Research England). We would like to thank Mr Timothy Dunstan for the acquisition of HRSEM images and EDX data.

References

1 C. Sevonius, P. Yrjas, D. Lindberg and L. Hupa, *Fuel*, 2019, **245**, 305–315.
2 D. Vamvuka, D. Zografos and G. Alevizos, *Bioresour. Technol.*, 2008, **99**, 3534–3544.
3 M. J. Taylor, H. A. Alabdrabalameer and V. Skoulou, *Sustainability*, 2019, **11**, 3604.
4 A. Grimm, M. Öhman, T. Lindberg, A. Fredriksson and D. Boström, *Energy Fuels*, 2012, **26**, 4550–4559.
5 W. Gao, M. Zhang and H. Wu, *Energy Fuels*, 2018, **32**, 3608–3613.
6 J. D. Morris, S. S. Daood, S. Chilton and W. Nimmo, *Fuel*, 2018, **230**, 452–473.
7 H. Chi, M. A. Pans, C. Sun and H. Liu, *Fuel*, 2019, **240**, 349–361.
8 M. J. Fernández, I. Mediavilla, R. Barro, E. Borjabad, R. Ramos and J. E. Carrasco, *Fuel*, 2019, **239**, 1115–1124.
9 T. Liliedahl, K. Sjöström, K. Engvall and C. Rosén, *Biomass Bioenergy*, 2011, **35**, S63–S70.
10 M. Balland, K. Froment, G. Ratel, S. Valin, J. Roussely, R. Michel, J. Poirier, Y. Kara and A. Galnares, *Waste Biomass Valorization*, 2017, **8**, 2823–2841.
11 S. Arvelakis, H. Gehrmann, M. Beckmann and E. G. Koukios, *Fuel*, 2003, **82**, 1261–1270.
12 P. Thy, B. M. Jenkins, R. B. Williams, C. E. Lesher and R. R. Bakker, *Fuel Process. Technol.*, 2010, **91**, 1464–1485.
13 P. Chaivatamaset, S. Tia, W. Methaviriyasilp and W. Pumisampran, *Waste Biomass Valorization*, 2018, 1–14, DOI: 10.1007/s12649-018-0358-y.
14 D. Lynch, A. M. Henihan, W. Kwapinski, L. Zhang and J. J. Leahy, *Energy Fuels*, 2013, **27**, 4684–4694.
15 M. Varol and A. T. Atimtay, *Bioresour. Technol.*, 2015, **198**, 325–331.

16 A. Burton and H. Wu, *Fuel*, 2016, **179**, 103–107.
17 B. Anicic, W. Lin, K. Dam-Johansen and H. Wu, *Fuel Process. Technol.*, 2018, **173**, 182–190.
18 B. Gatternig and J. Karl, *Biomass Convers. Biorefin.*, 2019, **9**, 117–128.
19 P. Chaivatamaset, S. Tia, W. Methaviriyasilp and W. Pumisampran, *Waste Biomass Valorization*, 2019, **10**, 3457–3470.
20 G. Olofsson, Z. Ye, I. Bjerle and A. Andersson, *Ind. Eng. Chem. Res.*, 2002, **41**, 2888–2894.
21 F. Scala, *Fuel Process. Technol.*, 2018, **171**, 31–38.
22 C. Sevonius, P. Yrjas and M. Hupa, *Fuel*, 2014, **127**, 161–168.
23 X. Xin, K. M. Torr, F. D. Mercader and S. S. Pang, *Energy Fuels*, 2019, **33**, 4254–4263.
24 R. Michel, J. Kaknics, E. de Bilbao and J. Poirier, *Ceram. Int.*, 2016, **42**, 2570–2581.
25 V. Mettanant, P. Basu and J. Butler, *Can. J. Chem. Eng.*, 2009, **87**, 656–684.
26 F. Duan, C.-S. Chyang, L.-h. Zhang and S.-F. Yin, *Bioresour. Technol.*, 2015, **183**, 195–202.
27 P. Chaivatamaset, P. Sricharoon, S. Tia and B. Bilitewski, *Appl. Therm. Eng.*, 2014, **70**, 737–747.
28 X. Qi, G. Song, S. Yang, Z. Yang and Q. Lyu, *Fuel*, 2018, **217**, 577–586.
29 F. Scala and R. Chirone, *Biomass Bioenergy*, 2008, **32**, 252–266.
30 R. Zhang, K. Lei, B. Q. Ye, J. Cao and D. Liu, *Bioresour. Technol.*, 2018, **268**, 278–285.
31 J. Marinkovic, H. Thunman, P. Knutsson and M. Seemann, *Chem. Eng. J.*, 2015, **279**, 555–566.
32 L. A. C. Tarelho, E. R. Teixeira, D. F. R. Silva, R. C. E. Modolo, J. A. Labrincha and F. Rocha, *Energy*, 2015, **90**, 387–402.
33 R. Fahmi, A. V. Bridgwater, L. I. Darvell, J. M. Jones, N. Yates, S. Thain and I. S. Donnison, *Fuel*, 2007, **86**, 1560–1569.
34 E. Brus, M. Öhman, A. Nordin, D. Boström, H. Hedman and A. Eklund, *Energy Fuels*, 2004, **18**, 1187–1193.
35 I. Vaskalis, V. Skoulou, G. Stavropoulos and A. Zabaniotou, *Sustainability*, 2019, **11**, 6433.
36 S. De Geyter, M. Öhman, D. Boström, M. Eriksson and A. Nordin, *Energy Fuels*, 2007, **21**, 2663–2668.
37 T. Ma, C. Fan, L. Hao, S. Li, P. A. Jensen, W. Song, W. Lin and K. Dam-Johansen, *Fuel Process. Technol.*, 2018, **180**, 130–139.
38 C. Zhou, C. Rosén and K. Engvall, *Appl. Energy*, 2016, **172**, 230–250.
39 A. Alper, *Phase Diagrams in Advanced Ceramics*, Osram Sylvania, Inc., 1995.
40 M. Öhman, L. Pommer and A. Nordin, *Energy Fuels*, 2005, **19**, 1742–1748.
41 J. Gómez-Hernández, D. Serrano, A. Soria-Verdugo and S. Sánchez-Delgado, *Chem. Eng. J.*, 2016, **284**, 640–649.
42 J. Pecho, T. J. Schildhauer, M. Sturzenegger, S. Biollaz and A. Wokaun, *Chem. Eng. Sci.*, 2008, **63**, 2465–2476.
43 V. Skoulou, E. Kantarelis, S. Arvelakis, W. Yang and A. Zabaniotou, *Int. J. Hydrogen Energy*, 2009, **34**, 5666–5673.
44 M. J. Taylor, H. A. Alabdrabalameer, A. K. Michopoulos, R. Volpe and V. Skoulou, *ACS Sustainable Chem. Eng.*, 2020, **8**, 5674–5682.
45 L. Deng, T. Zhang and D. Che, *Fuel Process. Technol.*, 2013, **106**, 712–720.
46 B. Gudka, J. M. Jones, A. R. Lea-Langton, A. Williams and A. Saddawi, *J. Energy Inst.*, 2016, **89**, 159–171.
47 A. Zabaniotou, V. Skoulou, G. Koufodimos and Z. Samaras, *Int. J. Chem. React. Eng.*, 2008, **6**, 1–19.
48 S. Kassaye, K. K. Pant and S. Jain, *Renewable Energy*, 2017, **104**, 177–184.
49 K. L. Chin, P. S. H'ng, M. T. Paridah, K. Szymona, M. Maminski, S. H. Lee, W. C. Lum, M. Y. Nurliyana, M. J. Chow and W. Z. Go, *Energy*, 2015, **90**, 622–630.

